

Investigation of topological and correlated materials by angular-resolved photoelectron spectroscopy

Jayita Nayak [#], Gerhard H. Fecher, Claudia Felser, Kai Filsinger, Jörg Fink, Nitesh Kumar, Kaustuv Manna, Chandra Shekhar, Yan Sun

The electronic-structure group of the solid-state chemistry department theoretically and experimentally investigates magnetic, correlated, and topological materials. Photoelectron spectroscopy is the most commonly used method to investigate electronic structures of materials. In many cases, it is suitable to directly compare the spectra with calculated electronic structures. Two energy ranges are important to distinguish between bulk and surface electronic structures. The sensitivity to bulk or surface properties is related to the energy dependence of the electron mean free path. Hard-X-ray photoelectron spectroscopy (HAXPES) provides insights into bulk electronic properties even for buried layers. We use this method to investigate not only thin films and multilayers but also bulk effects in topological materials. Low photon energies are suitable for angular-resolved photoelectron spectroscopy (ARPES). Its high energy and momentum (angular) resolutions establish it as a leading technique for analyses of electronic structures of all types of materials, including metals, narrow-band-gap semiconductors, superconductors, and in-situ-grown thin films. A major part of the studies on topological materials investigate their electronic structures by relating theory and experiments. Recently, we extensively studied various topological and correlated materials by photoelectron spectroscopy.

The electronic-structure group of the solid-state chemistry department extensively investigates electronic properties of various topological materials and superconductor families by employing angular-resolved photoelectron spectroscopy (ARPES). Since the discovery of topological insulators (TIs) and Fe-based high-temperature superconductors (FeSCs), studies of the electronic structures of these types of compounds have attracted significant attention owing to the high scientific importance related to new states of matter. Most important characteristics of TIs are topologically protected gapless states on their edges or surfaces and Dirac-cone-type dispersion of the topological surface states. In studies on novel materials with distinct topological properties, various new topological materials including Dirac semimetal and Weyl semimetal have been investigated.

We summarise some of our recent results obtained using the ARPES technique. Most of the ARPES measurements were performed at the UE112-PGM2b beamline of the synchrotron radiation facility BESSY (Berlin) using the 1^3 -ARPES end-station equipped with a Scienta R4000 energy analyser. All measurements were performed at a temperature of 1 K at various photon energies in the range of 50 eV to 110 eV using both horizontal and vertical polarisations. The total energy resolution was approximately 4 meV, while the angular resolution was 0.2° . Hard-X-ray photoelectron spectroscopy (HAXPES) was performed at the beamline BL47-XU, Spring-8 (Japan).

Investigation of the electronic structure of LaBi

Recently, the binary rare-earth-based monopnictide LaBi has attracted significant interest owing to its exotic magneto-transport properties including an extremely large and anisotropic magnetoresistance, similar to the materials that retain topological order. This stimulates studies of the electronic structure of this compound by ARPES to directly verify the existence of topological surface states.

In a recent study [1], our group reported the topological nature of LaBi by demonstrating the existence of three

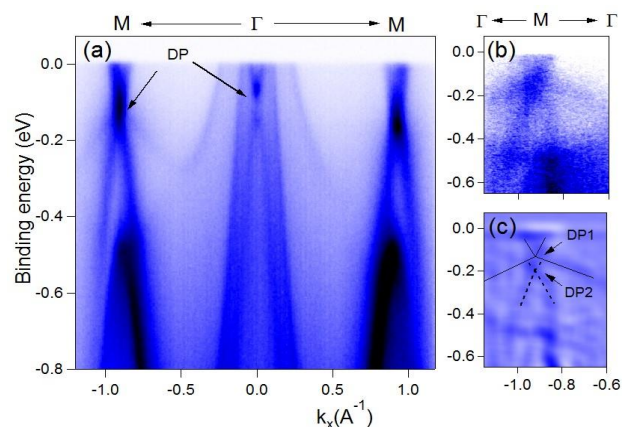


Fig.-1: (a) ARPES surface spectra measured along the $M-\Gamma-M$ direction with a photon energy of 83 eV. (b) Magnified images of the Dirac point at M measured along the $\Gamma-M-\Gamma$ direction. (c) Second derivative of the image in (b) to distinctly identify two Dirac points at M .

Dirac cones: two coexists at the corner and one at the centre of the Brillouin zone. In ARPES, the Dirac point at Γ appears at 150 meV below the Fermi energy (E_F), whereas the surface states at M are split into two Dirac points with energies of 123 meV and 198 meV below E_F . Moreover, we verified the surface nature of the Dirac states by a photon-energy-dependent ARPES measurement, which showed that the Dirac point did not change with the photon energy. The existence of an odd number of surface Dirac cones originates from the odd number of bulk band inversions, thus confirming the topological origin of the surface states. Our finding demonstrates that LaBi is a topological compensated semimetal, equivalent to a time-reversal-invariant topological insulator. It provides further insights into the topological surface states of the LaBi's semi-metallicity and related magneto-transport properties. Further details are provided in Reference [1].

Electronic structure of BaCr_2As_2

Recent experimental results indicate that Fe superconductors are moderately correlated systems. However, theoretical studies reported that owing to the multi-orbital electronic structure together with the Hund's exchange interaction J_H , correlation effects are important. According to the theoretical studies, the strongest correlation effects should be observed for compounds with an approximately half-filled $3d$ shell (e.g., Mn compounds and hole-doped ferropnictides). These effects should be smaller for compounds with a

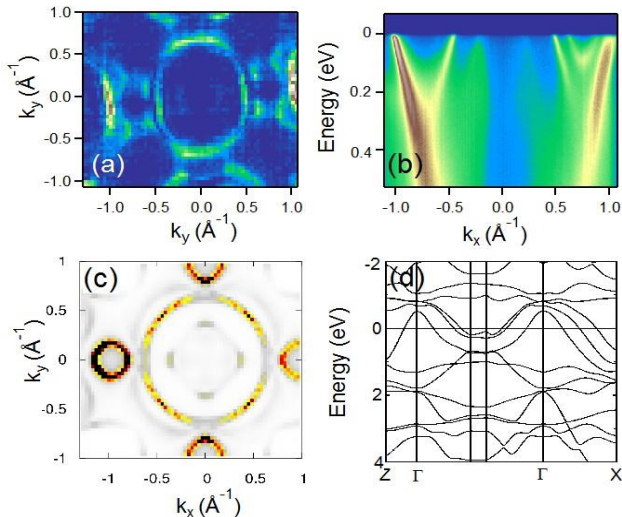


Fig.-2: ARPES results of BaCr_2As_2 using vertically (*s*) polarised photons with an energy of 88 eV yielding data in the $k_z = \pi/c$ plane. (a) Measured Fermi surface map and (b) energy distribution map along A-Z-A. (c) Photoemission calculation of the Fermi surface and (d) calculated band structure along X- Γ -M.

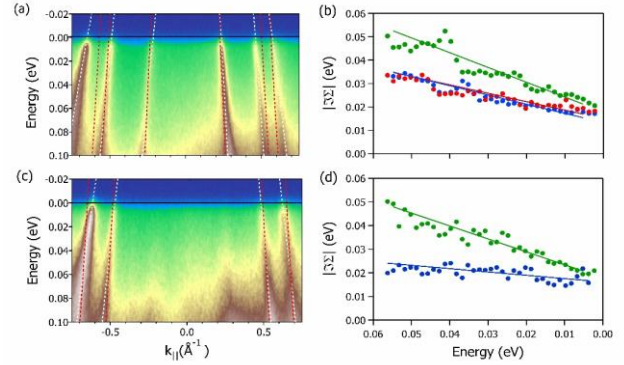


Fig.-3: Energy distribution maps and imaginary part of the self-energy obtained from ARPES experiments. (a) Map along the M- Γ -M direction, measured using *p*-polarised photons. (b) Imaginary part of the self-energy as a function of the energy for the three hole pockets, and linear fit; the red, blue, and green data points correspond to the three bands. (c,d) Similar plots as in (a,b), but acquired along the A-Z-A direction.

3d count closer to 6 (electron-doped ferropnictides) and compounds with a 3d count closer to 4 (e.g., chromiumpnictides). Therefore, we investigated whether the correlation effects are larger or smaller for pnictide compounds with 3d counts smaller than five.

By employing ARPES, we studied the three hole pockets at the centre (Γ point) and top (Z point) of the Brillouin zone (BZ) (see Fig. 2) [2]. By comparison with ab-initio band-structure calculation results, we obtain information on the correlation-induced mass renormalisation. Further information on the strength of correlation effects in BaCr_2As_2 are obtained from the lifetime broadening of the dispersions in the spectral function, as shown in Fig. 3. Compared to the hole-doped ferropnictides, the correlation effects in BaCr_2As_2 are considerably reduced. This can be explained by the theoretically predicted reduction in the effective on-site Coulomb interaction by the Hund's exchange interaction for compounds that do not have a half-filled $3d$ shell.

Electronic structure of CaAgAs

Early first-principle calculations on CaAgAs predicted a topological semi-metallic state for this compound. A nodal line should appear at the Fermi energy in the absence of spin-orbit coupling (SOC). When the spin-orbit interaction is considered, it transforms into a TI where the Fermi energy is positioned within the inverted band gap. However, the state of the material was not fully understood. Therefore, we performed calculations and spectroscopic investigations [3].

The calculated band structure showed the appearance of a nodal-line semi-metallic phase in the absence of SOC. The line node was centred on Γ for the directions ΓM and ΓK . The p_z orbital at the As atoms contributes mainly to the conduction band near Γ , whereas the valence band is formed from the p_x and p_y orbitals of As along with the s orbital of Ag. Therefore, band inversion occurs between the As p_x , p_y , and p_z orbitals. Further, SOC was used in the calculations to explain its influence on the nodal lines. The line nodes become gapped along the ΓM and ΓK directions and drive the system to the TI phase. This result indicates a non-trivial topology.

Fig. 4(a) shows the Fermi surface of CaAgAs measured with a photon energy of 85 eV. The Fermi surface appears as a circular hole pocket centred at Γ with $k_F = 0.2 \pm 0.02 \text{ \AA}^{-1}$. The red dotted box indicates the hexagonal surface BZ of CaAgAs; the high-symmetry points Γ , M , and K are marked. The calculated Fermi surface reproduces the experimental data after an energy shift of -0.5 eV from the charge neutral point (Figs. 4(b) and 4(c)). This shift is probably caused by a small self-doping. Approximately 0.1 electrons per unit cell need to be removed for the required shift in the Fermi energy. The ARPES band dispersion

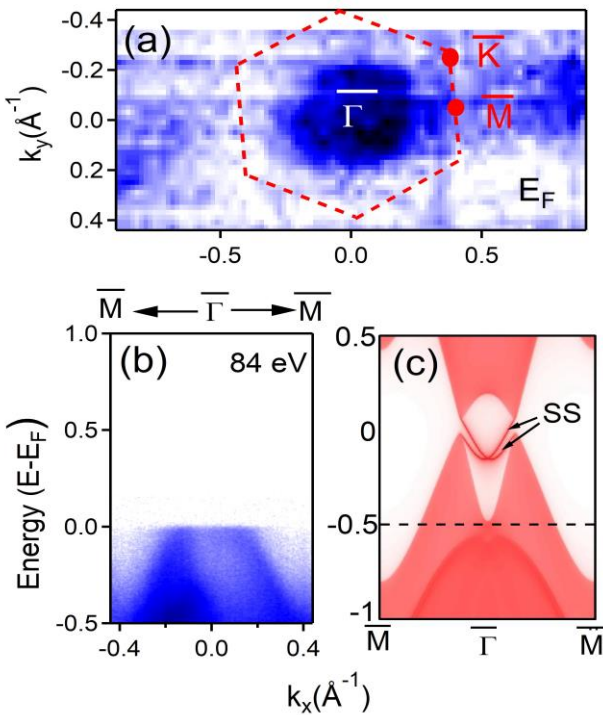


Fig.-4: Fermi surface of CaAgAs measured with a photon energy of 85 eV; the BZ and high-symmetry points are marked. (c) Constant-energy surface of CaAgAs at a binding energy of -0.35 eV .

(Fig. 4(b)) identifies the appearance of another hole-like band below 0.2 eV, positioned inside with respect to the outer hole-like band. It is worth noting that the inner band is also evident in the calculated spectra (Fig. 4(c)). In this context, another important observation is that both inner and outer bands (Fig. 4(b)) are asymmetric; the asymmetry is related to the matrix element effect in the photoemission, i.e., the intensity depends on the angle between the momentum of the outgoing electron and electric field vector of the photons. We performed photon-energy-dependent ARPES measurements in a wide photon energy range along the $M-\Gamma-M$ direction. Both inner and outer hole pockets centred at Γ significantly change with the photon energy, which indicates that the hole pockets originate from bulk bands. The observed strong dispersion with the photon energy is expected for bulk bands, whereas surface states should not disperse with the photon energy.

The electrical resistivity at 2 K is $7.4 \times 10^{-5} \Omega \cdot \text{cm}$. It decreases with the decrease in the temperature and saturates at a low temperature, typical for a metal, in contrast to the behaviour of TIs, where the Fermi energy should be inside the inverted band gap and the resistivity should increase with the decrease in the temperature with a plateau at low temperatures attributed to the topological surface states. The Hall resistivity $\rho_{yx}(B)$ demonstrates the existence of hole-type charge carriers owing to its positive slope. This is expected when the valence band crosses the Fermi energy, as verified by ARPES.

Bulk and surface electronic structures of the TI $\text{Bi}_2\text{Te}_2\text{Se}$

For $\text{Bi}_2\text{Te}_2\text{Se}$, manipulation of Dirac fermions through the temperature dependence of the chemical potential was investigated. Appearance of a bulk conduction band and consequently a remarkable shift of the Dirac point are observed at low temperatures (20 K), compared to the behaviour at high temperatures (200- 300 K). This was clearly revealed by HAXPES; therefore, it could be attributed to a pure bulk effect.

Fig. 5 compares temperature-dependent valence-band spectra in the region near E_F . A shift of the topmost valence states by approximately 100 meV is observed at 20 K, compared to 300 K. Simultaneously, the band edge shifts toward a higher binding energy, by 110 meV. Furthermore, an additional state seems to appear at 20 K, directly below E_F , which is not present in the spectra at 300 K.

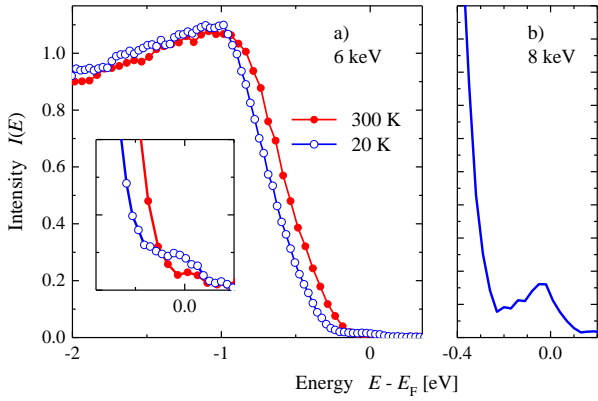


Fig.-5: Temperature-dependent $\text{Bi}_2\text{Te}_2\text{Se}$ HAXPES valence-band spectra. The spectra in (a) were obtained at 20 K and 300 K using a photon energy of 6 keV, while that in (b) was measured at 20 K and 8 keV.

The effect was also observed using ARPES where a temperature-induced shift of the Dirac cone was additionally observed.

Figs. 6(a) and 6(b) show the ARPES results. The momentum range covers the first and second BZs. The measurements at 200 K and 20 K are compared. The energy distribution curves (EDCs) recorded at 200 K exhibit a negligible spectral intensity at E_F . On the other hand, at 20 K, the spectral intensity is

significantly enhanced. The presence of a bulk band is evident at 20 K, whereas it is hardly observed in the spectra obtained at 200 K. In addition to the appearance of the bulk band, a shift of the band edge is observed, in agreement with the HAXPES measurement. The surface states are more pronounced in the 2nd BZ than in the first BZ, owing to the change in the angular distribution, caused by differences in the angular part of the photoemission matrix elements. Moreover, according to the valence-band edge shift, a shift of the Dirac point is observed between 200 K and 20 K.

The HAXPES and ARPES experiments are completely reversible, i.e., repeated cooling and heating of the sample up to room temperature recovers the original spectra. Both shift of the Dirac cone and appearance of bulk bands are related to a paradoxical shift in the chemical potential. Such bulk-related energy shifts have to be considered not only in photoelectron spectroscopy but also in analyses of other measurable physical quantities while designing devices for applications.

Therefore, the experimental results revealed temperature-dependent shifts in the spectral features in both bulk and surface-sensitive photoelectron spectroscopies using fast and slow electrons, respectively. The chemical potential, which defines the high-energy cut-off of the spectra, was located in the bulk conduction

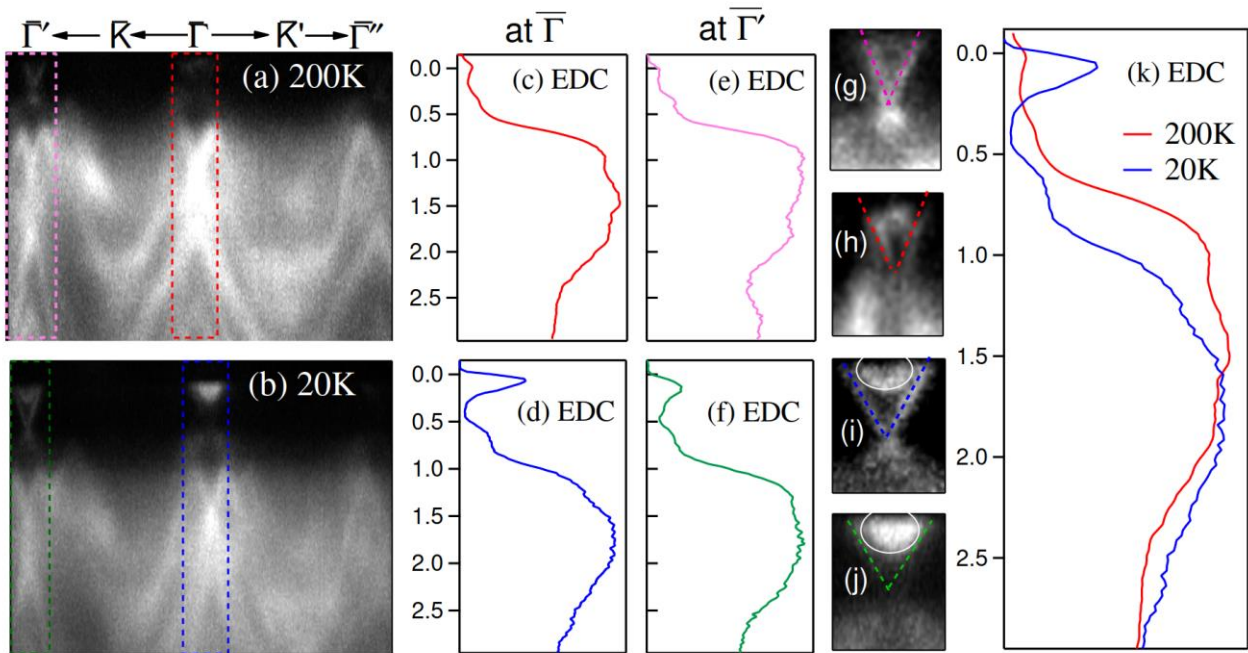


Fig.-6: ARPES of $\text{Bi}_2\text{Te}_2\text{Se}$ at (a) 200 K and (b) 20 K excited by Ge-I photons (21.2 eV). (c,e) and (d,f) EDCs for the areas marked in (a) and (b) plotted in the corresponding colors, respectively. (g,h) and (i,j) $E(k)$ distributions around the Γ -point of the second and first BZs near the Dirac point of the surface states in (a) and (b), respectively. (k) Direct comparison of the EDCs at 200 K and 20 K.

band at a low temperature, and shifted into the bandgap upon the increase in the temperature.

Outlook

Recently, the thin-film laboratory at the solid-state chemistry department was extended by introducing a combination of a molecular-beam-epitaxy (MBE) chamber with an ARPES end-station. This combination will enable in-situ investigations of topological materials grown as thin films by MBE with high qualities.

External Cooperation Partners

E. E. D. Rienks (IFW, Dresden, ARPES); J. Minár (Technical University of Munich, theory)

References

- [1]* *Multiple Dirac cones at the surface of the topological metal LaBi*, J. Nayak, S.-C. Wu, N. Kumar, C. Shekhar, S. Singh, J. Fink, E. E. D. Rienks, G. H. Fecher, S. S. P. Parkin, B. Yan and C. Felser, *Nature Communications* **8** (2017) 13942.
- [2]* *Observation of a remarkable reduction of correlation effects in BaCr₂As₂ by ARPES*, J. Nayak, K. Filsinger, G. H. Fecher, S. Chadov, J. Minár, E. E. D. Rienks, B. Büchner, J. Fink and C. Felser, *PNAS* **114** (2017) 12425.
- [3]* *Electronic properties of topological insulator candidate CaAgAs*, J. Nayak, N. Kumar, S.-C. Wu, C. Shekhar, J. Fink, E. E. D. Rienks, G. H. Fecher, Y. Sun and C. Felser, *J. Phys.: Condensed Matter* **30** (2018) 045501.

nayak@cpfs.mpg.de